

Performance Comparison of Converter Topologies for Double Fed Induction Generator-based Wind Energy Conversion Systems

Victor R. F. B. de Souza*, Luciano S. Barros**,
Flavio B. Costa*

* *Federal University of Rio Grande do Norte, RN, (e-mails: vicramoneng@gmail.com, flaviocosta@ect.ufrn.br)*

** *Federal University of Paraíba, PB, (e-mail: lsalesbarros@ci.ufpb.br)*

Abstract: The advancements in power electronics have supported the widespread penetration of wind energy conversion systems (WECS) in electric grids. In this context, power converters have crucial functionality in the control of active and reactive power injection, moreover they are directly related to voltage and current harmonic distortion levels, mechanical and thermal stress that are experienced by the wind turbine. Currently, several topologies have been tested in order to improve the performance and increase the power processing of WECS to support the network demand. Based on the relevance of this issue, this paper presents a performance comparison of a Double Fed Induction Generator (DFIG)-based WECS employing three topologies of back-to-back converters: two-level voltage source converter topology (2L-VSC), neutral point clamped (NPC) and modular multilevel converter (MMC). The analysis is accomplished considering DFIG currents, voltages, torque, speed and the total harmonic distortion (THD), highlighting the performance improvement employing multilevel topologies and the impacts of using each topology.

Keywords: DFIG-based wind energy conversion systems; performance comparison; two-level voltage source converter; three-level neutral point clamped; three-level modular multilevel converter.

1. INTRODUCTION

The wide penetration of WECS in electric grids has brought challenges to the power system, especially regarding to the reliability, efficiency and power quality of wind turbines (Infield and Freris, 2020). At the same time, advancements in power electronics have been permitting the implementation of more robust generators due to increased efficiency and power processing capability (Séguier and Labrique, 2012; Yazdani and Iravani, 2010). In this sense, DFIG is one of the most widely used generators in the wind energy market, representing over 50% of wind farm installations currently (Abad et al., 2011). The adoption of this technology was mainly due to its flexibility at variable speed, decoupled control operation of active and reactive power and the reduced volume of the power converter, usually 30% of the generator rated power (Abad et al., 2011; Sumathi et al., 2015). Traditionally, DFIG is used with a 2L-VSC back-to-back converter, one for the grid side (GSC) and another for the rotor side (RSC). The GSC has the function of controlling the dc-link voltage and reactive power delivered to the grid, while the RSC is responsible for the maximum power point tracking (MPPT) of the wind turbine. However, the use of two-level topology has technical limitations, with higher harmonic distortion, the need of switches with the bus rated voltage, and consequently with larger losses (Séguier and Labrique, 2012).

Development of new converter topologies has been leading to the reduction of losses, improving of power quality and increasing of the power processing capability. In this context, multilevel converters have stood out due to their capability to distribute voltage on power switches and to synthesize more output voltage levels. These features improve the reduction of voltage and current distortions, in addition to the equity of losses on switches with lower thermal stress (Bollen and Hassan, 2011; Dugan et al., 1996; Gupta and Bhatnagar, 2017). From the machine point of view, the choice of a back-to-back topology reflects directly on the electrical, thermal and mechanical features (Ma, 2015). Reduction in internal losses due to hysteresis, conductor overheating and electromagnetic torque oscillations increase the life of the gearbox coupled to the wind turbine (Vijeh et al., 2019; Abdelbaset et al., 2018). At the industrial level, the main multilevel topologies used for several applications are NPC (Nabae et al., 1981), flying capacitors (FC) (Meynard and Foch, 1992), and cascade H-bridges (CHB) (Mcmurray, 1971). The NPC topology is composed of clamping diodes that fix voltage levels through the connection with the DC bus central point. The FC uses capacitors instead of clamping diodes. The CHB uses H-bridges associated in series in order to synthesize voltage levels, with independent voltage sources. Recently, one topology that has stood out with half-bridge submodules is the MMC, which has been promising for

back-to-back use in WECS due to its high modularity and expansion flexibility (Lesnicar and Marquardt, 2003; Du et al., 2017).

In Hossain et al. (2018), multilevel topologies were employed for a comparative analysis of transient stability during a voltage sag using a DFIG-based WECS, between a 3L-NPC, 2L-VSC, and a 3L-FC, observing the improved transient response during a grid fault. The results presented a fast reestablishment to the pre-fault period with improved controllability.

Hossam-Eldin et al. (2020) presented a comparison using an NPC converter with different numbers of levels and employing two modulation techniques, the sinusoidal pulse width modulation (SPWM) and third harmonic injection pulse width modulation (THIPWM) under different wind speeds. The increase of the number of levels combined with the THIPWM technique obtained the best performance, reducing the THD of the DFIG.

Ouadi et al. (2017) presented a non-linear control implementation using the DFIG-based WECS with a 3L-NPC in the GSC for active filtering. Simulations under different wind speeds, voltage sags and frequency deviations demonstrated that the implemented system improved the performance using a multilevel topology in the GSC.

Merahi et al. (2014) presented a DFIG-based wind farm implementation using a 5L-NPC GSC. The converter feeds the four 2L-VSC connected to generators through the four available capacitors, eliminating the transformer between the generator and the grid. The control is performed by means of a supervisory algorithm that controls the DC bus voltages. In addition, the RSC controls are made separately for the 2L-VSC converters, employing the conventional vector control in $dq0$ coordinates, and a hysteresis current control for the GSC employing the 5L-NPC in order to control the active and reactive power of each generation unit. Simulation results have shown that the supervision algorithm was effective to control the generated power. In addition, the 5L-NPC topology provided cost reduction with only one GSC converter instead of four 2L-VSC converters.

Morais et al. (2017) presented a comparison between two structures using 3L-NPC, a conventional three-branch structure (3L-NPC-3B), and a two-branch structure (3L-NPC-2B). The performance of both was evaluated to verify the feasibility of replacing the standard structure with the 3L-NPC-2B. The results demonstrated the applicability of the 3L-NPC-2B, showing a reduction of performance compared to the 3L-NPC due to the limited structure of the two-branch topology. The control of active and reactive power and electromagnetic torque presented larger oscillations. However, in some phases the 3L-NPC-2B structure presented lower harmonic distortion, which means it can improve the power quality.

Sujod and Erlich (2013) presented a comparison of harmonics and common mode voltage, this voltage is generated between the neutral point of the load and the ground, leading to current distortion disturbances in the machine windings for 3L-NPC and 2L-VSC back-to-back in a DFIG-based WECS. Two modulation techniques were employed: the phase opposition disposition (POD-PWM)

and phase disposition (PD-PWM). The results demonstrated that the common mode voltage is reduced by 66% employing the 3L-NPC with the POD technique.

Merahi and Berkouk (2013) presented a new method to establish the voltage balance of capacitors of a 5L-NPC connected to a DFIG-based WECS. The voltage control is performed by means of two loops, in which the first one controls the average voltage value of the capacitors and the second controls the voltage difference in each half arm of the converter employing a voltage clamping bridge. The results demonstrated that the used control method minimized oscillations in the DC bus.

Based on the relevance of this context, this paper deals with a comparative approach in the back-to-back converters of a DFIG-based WECS using three topologies, which are 2L-VSC, 3L-NPC and 3L-MMC. The analysis demonstrates the internal structural aspects of the pair of converters as well as the impacts on the generator, by verifying currents, voltages and electromagnetic torque of DFIG. The results demonstrate superior performance in current distortions, DC bus and torque oscillation employing the MMC topology. This work is divided as follows: section II presents the DFIG-based WECS implemented; section III presents the three converter topologies; section IV presents the obtained results; and at the final it presents the conclusions.

2. DFIG-BASED WECS IMPLEMENTED

The implemented system consists of a DFIG-based WECS with two back-to-back converters sharing the same DC bus and connected through the common coupling point (PCC) to a three-phase grid. Fig. 2 depicts the system architecture. In this scenario, the DFIG is modeled using the abc coordinate system, and the converters use IGBT's as power switch (Abad et al., 2011). The control system implemented for the DFIG was realized in the synchronous reference $dq0$ using PI controllers for the direct axis and quadrature loops (Abu-Rub et al., 2014). For the comparative analysis, the three abovementioned back-to-back converter topologies are used in the DFIG-based WECS. In order to ensure an adequate comparison, the same control structure with their respective modulation techniques are considered for each converter.

3. BACK-TO-BACK CONVERTER TOPOLOGIES

The structures of 2L-VSC, 3L-NPC, and 3L-MMC employed in the study are depicted in Fig. 3. Details of the presented topologies and the possible switching combinations with their respective output voltages are shown in (Abu-Rub et al., 2014). Among the topologies presented, the MMC presents a particularly modular structure with the capability of synthesizing the output voltages by means of the sum of the active submodules per converter arm. Representing the active submodules by means of a switching function, it is possible to relate states of the submodules switches with capacitor voltages and output voltages, thus:

- If $S1 = 1$ and $S2 = 0$, $V_{cap} = \text{ON}$;
- If $S1 = 0$ and $S2 = 1$, $V_{cap} = \text{OFF}$;
- Else $V_{cap} = \text{OFF}$.

The capacitor submodule average voltage is given by:

$$V_{cap} = \frac{V_{bus}}{N_{SM}}, \quad (1)$$

where N_{SM} is the number of active submodules per arm and the number of output voltage levels is given by $N_{SM} + 1$. Each arm in the MMC can be represented by a controlled voltage source, with magnitude given by:

$$V_{arm} = \frac{SM_{active} V_{bus}}{N_{SM}}, \quad (2)$$

where SM_{active} is the number of active submodules. Considering V_{SM} the submodule voltage which is the capacitor voltage, the converter arm voltage is a function of the number of submodules, inductance, and resistance arm as follows:

$$V_{arm} = \sum_{n=0}^n V_{SM} + L_{arm} \frac{di_{arm}}{dt} + R_{arm} i_{arm}. \quad (3)$$

Thus, the output voltage levels of the MMC are given by the sum of the submodule voltage in the arm (Byung Moon Han and Jong kyou Jeong, 2014). In addition, an classification algorithm is used for the voltage balancing of the MMC. The schematic diagram is depicted in Fig. 1.

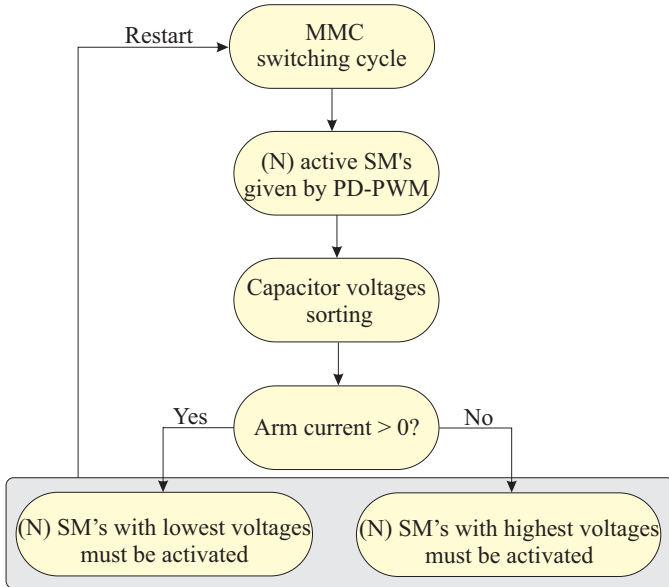


Figure 1. MMC capacitor voltage balancing algorithm.

For the 2L-VSC converter, SPWM technique was used, where a triangular carrier is compared to the three-phase reference voltages for the switch pulse generator (Abad et al., 2011). For the 3L-NPC and 3L-MMC multilevel topologies, the PDPWM technique was employed, which is also based on triangular carrier, with the number of carriers N_{tri} defined by $N-1$, where N is the number of converter levels. In this modulation scheme the carriers are shifted in level, having the same amplitude and in phase with each other (Abu-Rub et al., 2014).

4. SIMULATIONS AND RESULTS

Matlab/Simulink platform was used to the DFIG-based WECS simulation implementation. The system and DFIG parameters are shown in Table 1. In order to compare the three converter topologies, stator currents (I_S), rotor currents (I_R), electromagnetic torque (T_E), DC bus voltage (V_{BUS}) and total harmonic current distortion for I_S and I_R were analyzed. The results obtained using 2L-VSC, 3L-NPC and 3L-MMC back-to-back topologies are shown in Fig. 3.

Table 1. System and DFIG Parameters

Parameter	Value
Nominal voltage	311/220 V
Stator voltage	311 V
Stator frequency	60 Hz
Nominal power	3400 W
Switching frequency	5 kHz
DC bus voltage	600 V
Submodule capacitance	3000 μF
C_{BUS}	3000 μF
L_{arm}	1 mH
R_{arm}	0.5 Ω
L_s	0.214067 H
L_r	0.214067 H
R_s	2.8237 Ω
R_r	2.8237 Ω
L_m	0.29835 H
P_p	2
Fm	0.00146 N-m-s/rad
M_s	-0.0994 H
M_r	-0.0994 H
M_{sr}	0.1989 H
J_m	0.0133 Kg.m ²

4.1 Back-to-Back 2L-VSC Topology

Considering DFIG-based WECS employing back-to-back 2L-VSC topology, I_S does not have high distortions, presenting a sine-shaped pattern with low THD_{I_S} of 2.56%. However, the waveforms of I_R indicate a larger harmonic distortion, with THD_{I_R} of 8.34%, leading to a reduction in DFIG efficiency during the generation process, as well as directly impacting the internal loss rates of the generator. On the other hand, low oscillation around V_{BUS} was verified with 0.16% of the reference value. In addition, the behavior of T_E was evaluated, where it was verified oscillations in steady-state. This issue can generate losses due to friction, mechanical stress and shorter life of the gearbox due to vibrations in the DFIG shaft.

4.2 Back-to-Back 3L-NPC Topology

The 3L-NPC back-to-back topology reduced the THD_{I_S} in 49.60%, being 1.29%. In addition, the THD_{I_R} obtained a better performance, being 5.01%, representing a reduction of 39.92%. The value of V_{BUS} in comparison to 2L-VSC also showed less oscillation around the nominal value 0.5 V, representing a reduction of 50%. Regarding the T_E in steady-state, it is observed that there was a reduction of torque oscillations in the DFIG shaft, which reflects in the preservation of the lifetime of the gearbox, as well as the internal mechanical structure of the DFIG.

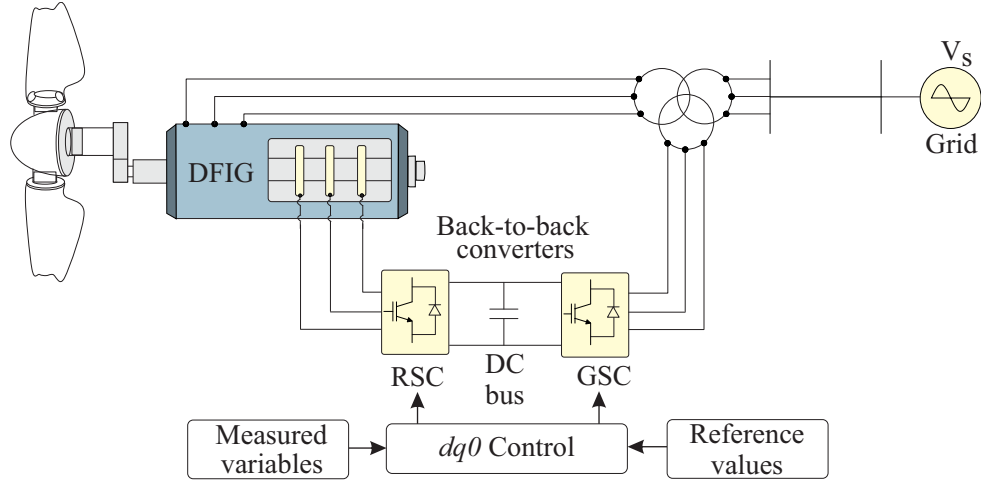


Figure 2. DFIG-based WECS implemented.

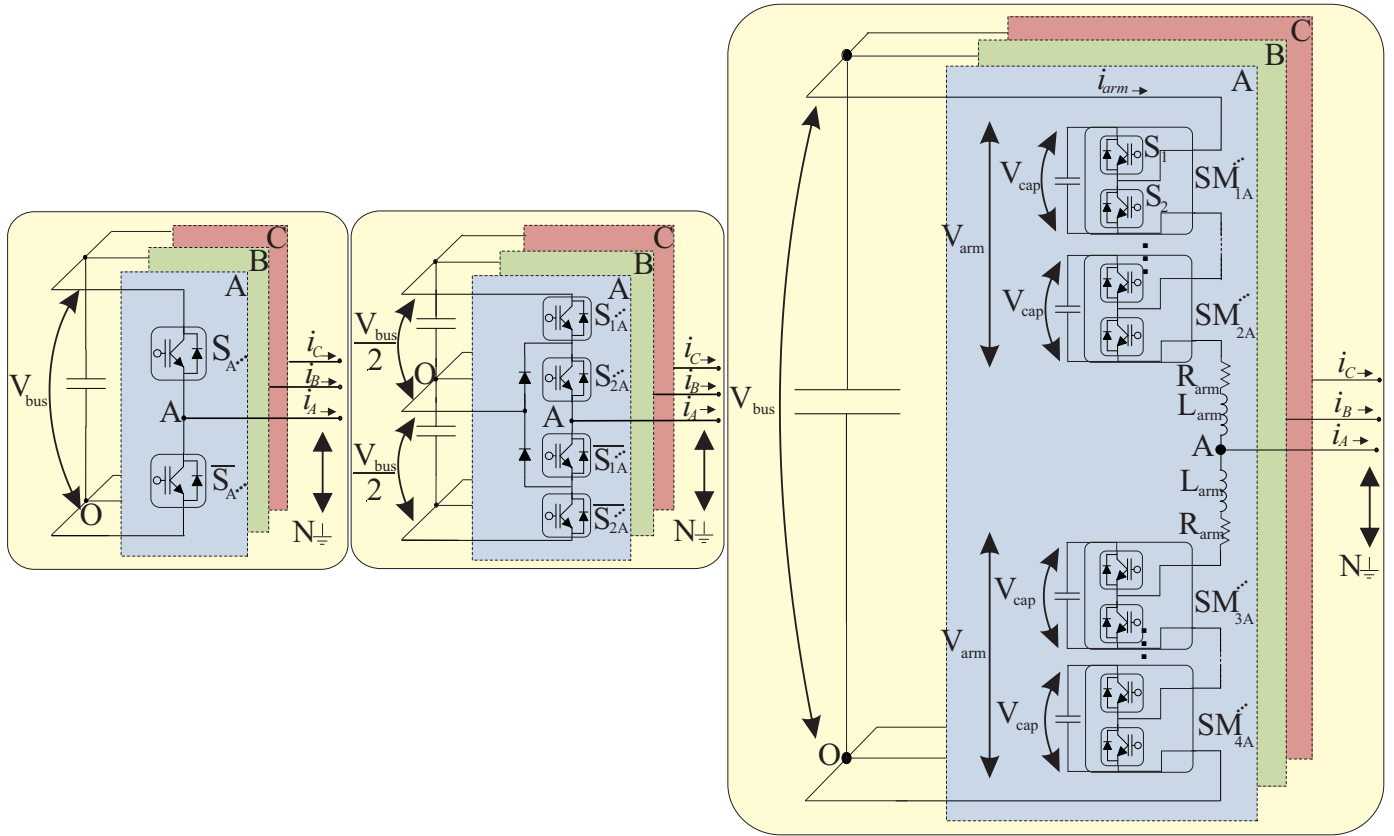


Figure 3. Three-phase back-to-back converter topologies: 2L-VSC, 3L-NPC, and 3L-MMC.

4.3 Back-to-Back 3L-MMC Topology

The 3L-MMC back-to-back topology presented similar performance to 3L-NPC with some variations. There was a slight increase in THD_{IS} being 1.59%, as well as verified in THD_{iR} , being 5.32%. This result is due to the larger amount of capacitors present in the submodules that compose the structure of the MMC, representing no significant performance reduction. On the other hand, V_{BUS} presented the smallest oscillation around the nominal value in the steady-state, with 0.3 V. In addition, the behavior of T_E showed low oscillation levels with values close to the

3L-NPC topology, allowing the reduction of internal losses and providing greater efficiency to the DFIG.

4.4 Comparison of 2L-VSC, 3L-NPC, and 3L-MMC Back-to-Back Topologies

Based on the results obtained from DFIG-based WECS using 2L-VSC, 3L-NPC and 3L-MMC, it is possible to highlight the characteristics of the back-to-back set for the three cases using the same control structure. The 2L-VSC provided the largest harmonic distortion, besides the largest oscillation in V_{BUS} , as well as in T_E . This

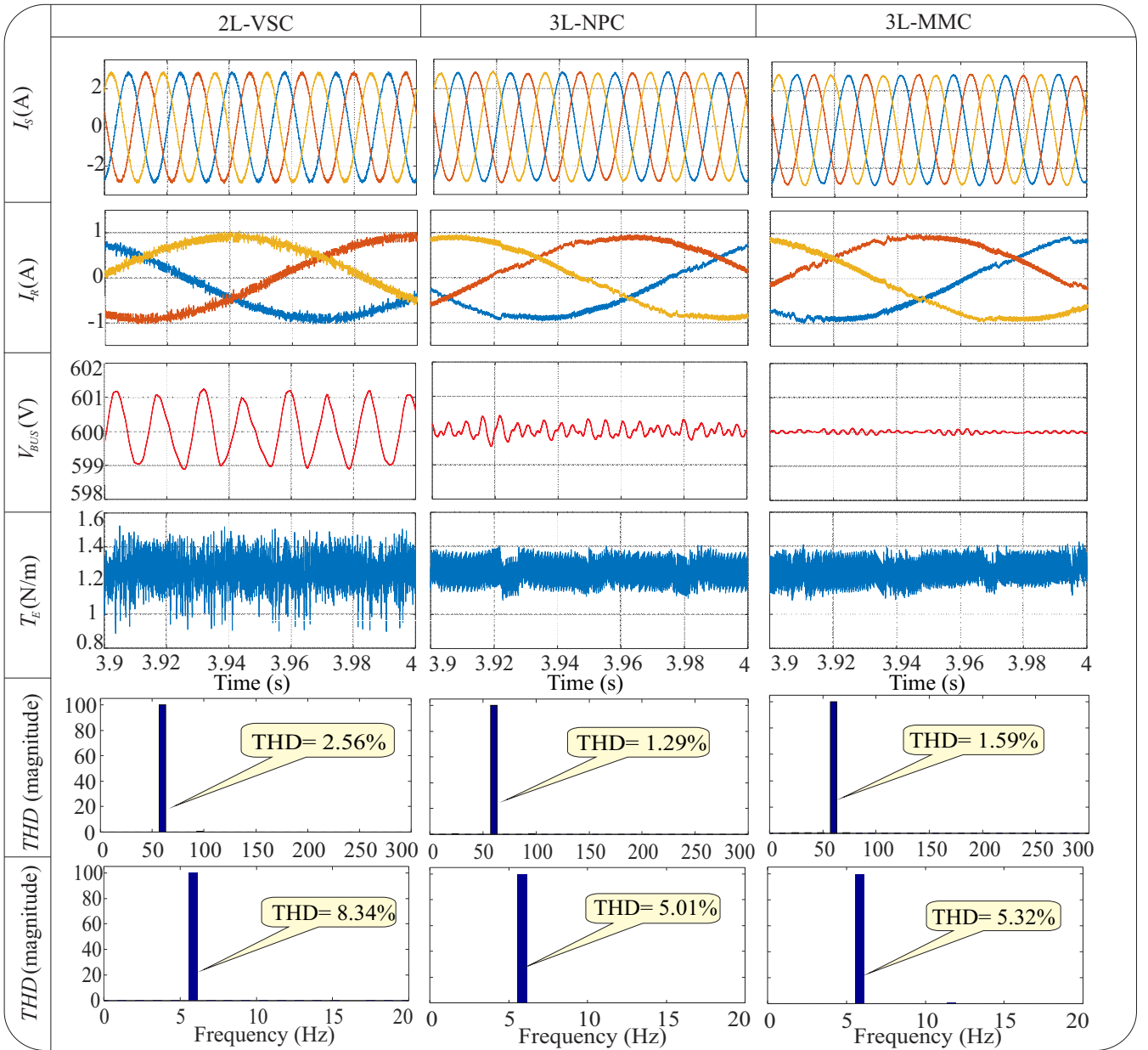


Figure 4. Obtained results for DFIG-based WECS back-to-back 2L-VSC, 3L-NPC, and 3L-MMC.

is due to the structural aspects of the converter and the limitation of synthesizing the output voltage levels, which generates higher levels of losses and harmonic distortion in the DFIG, as well as higher stress in the internal switches of the GSC and RSC converters. The 3L-NPC topology presented a significant improvement for the harmonic distortion rates, minimizing oscillations in DC bus and electromagnetic torque, due to the increase in the number of converter levels. However, the NPC requires the use of clamping diodes to fix voltage levels, besides having the inconvenience of unequal losses in the semiconductors with the increase in the number of levels, leading to the series association of diodes for a better voltage distribution. The 3L-MMC topology also presented a good performance, although having a lower performance than the NPC, it obtained lower oscillations in the voltage V_{BUS} . In despite of the need to use a voltage balancing algorithm for the

submodule capacitors, its modular characteristic presents a structural technical advantage in comparison to the other topologies, with easy expansion of the number of levels, losses equally distributed in the submodules and without the need to use clamping diodes. In addition, performance improvement can be achieved by increasing the number of levels. These characteristics bring more reliability and robustness to the MMC in DFIG-based WECS.

5. CONCLUSIONS

This paper presented a Double Fed Induction Generator-based Wind Energy Conversion System using three types of back-to-back converter topologies: two-level voltage source converter, three-level neutral point clamped, and three-level modular multilevel converter. The use of multilevel topologies provided a better performance regarding the conventional topology. The lower complexity level of

conventional topology implementation limits the structure of converters with regards to the level of the total harmonic distortion, voltage oscillation in the continuous current bus and electromagnetic torque. All these variables directly spoil the behavior during generation, deteriorating the current waveforms in the stator and rotor, affecting the mechanical characteristics in relation to the machine shaft and gearbox. On the other hand, the use of three-level neutral point converter provided a better response among the presented topologies, with the lowest total harmonic distortion considerably, improving the aspect of the currents in steady-state. However, the neutral point clamped topology has a complex structure, with unequal losses in semiconductors, and requires the association of clamping diodes, leading to a higher final implementation cost. The three-level modular multilevel, besides presenting higher implementation complexity and a slightly low performance than neutral point topology, has a flexible structure with easy expansion, which can be implemented with lower costs for a higher number of levels, thus overcoming the performance due to the inexistence of clamping diodes. This comparative study contributed to verify the main impacts of using back-to-back multilevel topologies, providing an adequate choice of converters in face of the great expansion of wind power generation.

ACKNOWLEDGMENT

This work was supported by the National Council for Scientific and Technological (CNPq) and by the Coordination for the Improvement of Higher Education Personnel (CAPES), Brazil.

REFERENCES

- Abad, G., Lopez, J., Rodriguez, M., Marroyo, L., and Iwanski, G. (2011). *Doubly fed induction machine: modeling and control for wind energy generation*, volume 85. John Wiley & Sons.
- Abdelbaset, A., Mohamed, Y.S., El-Sayed, A.H.M., and Ahmed, A.E.H.A. (2018). Wind driven doubly fed induction generator. *Grid Synchronization and Control*.
- Abu-Rub, H., Malinowski, M., and Al-Haddad, K. (2014). *Power electronics for renewable energy systems, transportation and industrial applications*. John Wiley & Sons.
- Bollen, M.H. and Hassan, F. (2011). *Integration of distributed generation in the power system*, volume 80. John Wiley & Sons.
- Byung Moon Han and Jong kyou Jeong (2014). Switching-level simulation model of mmc-based back-to-back converter for hvdc application. In *2014 International Power Electronics Conference (IPEC-Hiroshima 2014 - ECCE ASIA)*, 937–943.
- Du, S., Dekka, A., Wu, B., and Zargari, N. (2017). *Modular multilevel converters: analysis, control, and applications*. John Wiley & Sons.
- Dugan, R.C., McGranaghan, M.F., and Beaty, H.W. (1996). *Electrical power systems quality*. New York, NY: McGraw-Hill, | c1996.
- Gupta, K.K. and Bhatnagar, P. (2017). *Multilevel inverters: conventional and emerging topologies and their control*. Academic Press.
- Hossain, B., Rahman, H., and Islam Sheikh, R. (2018). Transient stability analysis of a dfig-based wind turbine using three level npc converter. In *2018 International Conference on Computer, Communication, Chemical, Material and Electronic Engineering (IC₄ME₂)*, 1–4.
- Hossam-Eldin, A.A., Negm, E., Elgamal, M.S., and Abo-Ras, K.M. (2020). Operation of grid-connected dfig using spwm- and thipwm-based diode-clamped multilevel inverters. *IET Generation, Transmission Distribution*, 14(8), 1412–1419.
- Infield, D. and Freris, L. (2020). *Renewable energy in power systems*. John Wiley & Sons.
- Lesnicar, A. and Marquardt, R. (2003). An innovative modular multilevel converter topology suitable for a wide power range. In *2003 IEEE Bologna Power Tech Conference Proceedings*, volume 3, 6–pp. IEEE.
- Ma, K. (2015). *Power electronics for the next generation wind turbine system*, volume 5. Springer.
- Mcmurray, W. (1971). Fast response stepped-wave switching power converter circuit. US Patent 3,581,212.
- Merahi, F. and Berkouk, E.M. (2013). Back-to-back five-level converters for wind energy conversion system with dc-bus imbalance minimization. *Renewable Energy*, 60, 137 – 149.
- Merahi, F., Berkouk, E.M., and Mekhilef, S. (2014). New management structure of active and reactive power of a large wind farm based on multilevel converter. *Renewable energy*, 68, 814–828.
- Meynard, T. and Foch, H. (1992). Multi-level choppers for high voltage applications. *EPE journal*, 2(1), 45–50.
- Morais, E.E.C., de A. Lima, F.K., and Branco, C.G.C. (2017). Comparison between three-phase structures of two and three branches with ancillary services capabilities in type-3 wind turbines: Npc topology. In *2017 IEEE 8th International Symposium on Power Electronics for Distributed Generation Systems (PEDG)*, 1–7.
- Nabae, A., Takahashi, I., and Akagi, H. (1981). A new neutral-point-clamped pwm inverter. *IEEE Transactions on industry applications*, (5), 518–523.
- Ouadi, H., Barra, A., and Khalid, E.M. (2017). Nonlinear control for grid connected wind energy system with multilevel inverter. *Journal of Engineering and Applied Sciences*, 12, 1171–1188.
- Séguier, G. and Labrique, F. (2012). *Power electronic converters: DC-AC conversion*. Springer Science & Business Media.
- Sujod, M.Z. and Erlich, I. (2013). Harmonics and common mode voltage in a dfig with two-level and three-level npc converter using standard pwm techniques. In *IECON 2013 - 39th Annual Conference of the IEEE Industrial Electronics Society*, 1650–1655.
- Sumathi, S., Kumar, L.A., and Surekha, P. (2015). Wind energy conversion systems. In *Solar PV and Wind Energy Conversion Systems*, 247–307. Springer.
- Vijeh, M., Rezanejad, M., Samadaei, E., and Bertilsson, K. (2019). A general review of multilevel inverters based on main submodules: Structural point of view. *IEEE Transactions on Power Electronics*, 34(10), 9479–9502.
- Yazdani, A. and Iravani, R. (2010). *Voltage-sourced converters in power systems: modeling, control, and applications*. John Wiley & Sons.